



Neuroepithelial Body Microenvironment Is a Niche for a Distinct Subset of Clara-Like Precursors in the Developing Airways

Citation

Guha, Arjun, Michelle Vasconcelos, Yan Cai, Mitsuhiro Yoneda, Anne Hinds, Jun Qian, Guihua Li, et al. 2012. Neuroepithelial Body Microenvironment Is a Niche for a Distinct Subset of Clara-Like Precursors in the Developing Airways. *Proceedings of the National Academy of Sciences* 109, no. 31: 12592–12597.

Published Version

doi:10.1073/pnas.1204710109

Permanent link

<http://nrs.harvard.edu/urn-3:HUL.InstRepos:12872181>

Terms of Use

This article was downloaded from Harvard University's DASH repository, and is made available under the terms and conditions applicable to Other Posted Material, as set forth at <http://nrs.harvard.edu/urn-3:HUL.InstRepos:dash.current.terms-of-use#LAA>

Share Your Story

The Harvard community has made this article openly available.
Please share how this access benefits you. [Submit a story](#).

[Accessibility](#)

Major: Biology Minor: Developmental Biology

The neuroepithelial body microenvironment is a niche for a distinct subset of Clara-like precursors in the developing airways

Arjun Guha^{1*}, Vasconcelos M.^{1*}, Cai, Y.³, Yoneda, M.³, Hinds A.¹, Qian J.¹, Li, G.¹, Dickel L.², Johnson J.², Kimura, S.³, Guo., J.⁴, McMahon, J.⁴, McMahon, A.⁴, and Wellington V. Cardoso¹

¹Pulmonary Center, Boston University School of Medicine,
Boston, MA 02118

² Department of Neuroscience, UT Southwestern Medical Center,
Dallas, TX75390

³ Laboratory of Metabolism, National Cancer Institute,
Bethesda, MD 20892

⁴Department of Molecular and Cell Biology, Harvard University,
Cambridge, MA 01238

* co-first authors

Keywords: Notch signaling, Neuroepithelial body, Clara cell, Ascl1, lung development

Running title: Neuroepithelial body microenvironment and secretory cell precursors

Corresponding authors:

Wellington V. Cardoso, MD, PhD,
Professor of Medicine and Pathology,
Pulmonary Center - Boston University School of Medicine,
72 East Concord Street, R-304,
Boston, MA, 02118.
Tel: 617-638-6198;
Fax: 617-536-8093;
E-mail: wcardoso@bu.edu

Arjun Guha, PhD
Assistant Professor of Medicine
Pulmonary Center, Boston University School of Medicine,
72 East Concord Street R-304,
Boston, MA 02118
Phone: (617) 638-6198
Fax : (617) 536-8093
e-mail: aguha@bu.edu

ABSTRACT

Clara cells of mammalian airways have multiple functions and are morphologically heterogeneous. While Notch signaling is essential for the development of these cells, it is unclear how Notch influences Clara cell specification and if diversity is established among Clara cell precursors. Here we identify expression of the secretoglobin *Scgb3a2* and Notch activation as early events in a program of secretory cell fate determination in developing murine airways. We show that *Scgb3a2* expression *in vivo* is Notch-dependent at early stages, is ectopically induced by constitutive Notch1 activation, and that *in vitro* Notch signaling together with the pan-airway transcription factor Ttf1 (Nkx2.1) synergistically regulate secretoglobin gene transcription. Furthermore, we identified a novel subpopulation of secretory precursors juxtaposed to presumptive Neuroepithelial Bodies (NEBs), distinguished by their strong *Scgb3a2* and Uroplakin3A (*Upk3a*) signals and reduced Ccsp (*Scgb1a1*) expression. Their association with NEBs is crucial, since genetic disruption of *Ascl1* prevented NEB formation and selectively interfered with formation of this subpopulation of cells. Lineage labeling of Upk3A-expressing cells during development showed that these cells remain uncommitted during embryonic development and contribute to Clara and ciliated cells in the adult lung. Together our study suggests a role for Notch in the induction of a Clara cell-specific program of gene expression and reveals that the NEB microenvironment in the developing airways is a niche for a distinct subset of Clara-like precursors.

\body

INTRODUCTION

The airways of the mammalian lung are populated by distinct epithelial cell types distinguished by their morphology and expression of molecular markers. Clara and ciliated cells are the most abundant while basal and neuroendocrine (NE) cells are restricted in number and distribution (1). Clara cells synthesize components of the airway lining fluid, mediate mucociliary clearance in concert with ciliated cells, and metabolize environmental toxins. Furthermore, they act as facultative progenitor cells during lung injury-repair (1-3).

Clara cells in the mouse lung have been distinguished in molecular terms by the expression of the secretoglobin *Scgb1a1*/Clara cell secretory protein (Ccsp or CC10). Subpopulations of Clara cells with distinctive morphology and susceptibility to environmental exposures have been reported in the mouse lung and in other species (4). For example, ultrastructural analysis of conducting airways shows that Clara cells surrounding clusters of neuroepithelial cells (neuroepithelial bodies, NEBs) have a distinct flattened morphology (5). These cells are also functionally distinct from other Clara cells as they are deficient in the cytochrome P450 enzyme *Cyp2f2* (6). It is thought that the absence of *Cyp2f2* renders resistance to Naphthalene injury (6).

Genetic studies in mice demonstrate an essential role for the Notch signaling in the specification of Clara cells during lung development (7, 8). The Notch pathway is a juxtacrine signaling system that regulates cell fate choices in multiple biological systems (9-11). The pathway is activated by the binding of transmembrane Notch receptors (Notch1-4) and transmembrane ligands Delta-like (Dll1, 3, 4) or Jagged (Jag1, Jag2). Ligand- receptor interaction results in gamma-secretase-dependent cleavage of the cytoplasmic domain of the Notch receptor. Nuclear translocation and interaction of this cleaved intracellular domain (NICD) with the Rbpjk transcriptional complex then leads to activation of a canonical pathway and the expression of target genes. Developing airways that are deficient in Rbpjk or Protein O-fucosyltransferase-1 (*Pofut1*), an enzyme required for the efficient binding of Notch receptor to ligand, lack Clara cells and have supernumerary ciliated cells (7, 8). Conversely, constitutive activation in the developing lung epithelium results in mucous metaplasia and in a decrease in numbers of ciliated cells (12).

Studies of the mechanisms of Clara cell specification and the role of Notch signaling therein have been limited by the paucity of early markers of differentiation. Transcription factors that label ciliated (*Foxj1*), neuroendocrine (*Ascl1*) and basal (*Trp63*) progenitors are known. However, with the exception of NICD, no nuclear factor specific to Clara cell progenitors has been identified. *Hes1*, a Notch transcriptional target, is expressed in developing airways, including Clara precursors, but it is not required for the specification of Clara cells (13). Secretoglobins are a family of small, secreted, structurally similar disulfide-linked dimers of which three members, Ccsp (*Scgb1a1*), *Scgb3a1* and *Scgb3a2* are expressed in Clara cells in the lung (14). At present, the secretoglobin Ccsp is the only definitive marker for Clara cells. Markers like *Trp63*, *Ascl1* and *Foxj1* have been localized to the developing airways E12.5 onwards. In contrast, Ccsp expression has been observed from E15.5 onwards (14).

Here we examine the early events associated with the induction of Clara cell fate and the contribution of developmental programming in establishing differences among Clara cells in the mouse airway epithelium. We identify *Scgb3a2* and activated Notch as markers of an early program of Clara cell fate. Moreover, we implicate Notch as a mediator of a Clara cell-specific

program of gene expression in airway epithelial precursors. This program is modified in the developing NEB microenvironment to generate a distinct subpopulation of Clara cell precursors.

RESULTS

Notch activation in the developing airways precedes expression of known markers of airway differentiation.

Lineage analysis of cells that experienced Notch1 activation in the developing airways and loss-of-function genetic studies have shown that Notch signaling correlates with and is essential for the Clara cell fate (7, 8). To characterize the spatio-temporal regulation of Notch signaling in the developing airways we examined the distribution of activated Notch1 by immunohistochemistry (IHC) using an antibody against cleaved Notch1 (hereafter NICD) (7). NICD labeling was first detected in the respiratory epithelium at E12.5, at low levels, and restricted to the trachea and main bronchi (Fig. 1A,B). At E14.5 NICD-positive cells were more abundant in the proximal airways but absent in the distal airways (Fig. 1C-E). At this stage strong NICD signals were detected in clusters occupying a relatively apical position within the pseudo-stratified epithelium in proximal intrapulmonary airways (Fig. 1E,F). This contrasted with lower intensity and more homogenous pattern of NICD labeling outside the clusters. The expression in clusters was reminiscent of the distribution of *Ascl1* (mouse achaete-scute complex homologue 1, *Mash1*), a bHLH transcription factor essential for NE cell fate and a marker for presumptive neuroepithelial bodies (pNEBs) (15). Double IHC confirmed the presence of the NICD clusters juxtaposed to and distinct from *Ascl1*-expressing cells (Fig. 1F). At this stage most, if not all, clusters of NICD were juxtaposed to pNEBs. By E18.5 NICD was detected throughout the airway epithelium and in clusters associated with pNEBs. (Fig. 1G). Previous studies have suggested that *Ascl1* (E13.5) is the earliest marker for airway differentiation (15). We conclude that Notch signaling is activated in the developing airway epithelium prior to any of the known markers of differentiation and is activated around pNEBs from early stages.

NEB-associated cells show distinct phenotypic features during development suggestive of a subpopulation of Clara cell precursors

The early onset of Notch activation in the developing lung suggested that the determination of the Clara cell fate initiates earlier than the expression of *Ccsp* and led us to search for early markers. Previous studies showed that *Scgb3a2*, another member of the secretoglobin gene family, is also expressed in secretory Clara cells of developing airways (8, 14, 16, 17). This led us to investigate whether *Scgb3a2* correlates with Notch activation at early stages. In situ hybridization (ISH) revealed *Scgb3a2* expression from E12.5 onwards; expression was localized to the trachea and extrapulmonary bronchi (Fig. 2A). *Scgb3a2* expression became stronger and expanded to lobar bronchi at E13.5-14.5 and was widespread by E18.5 (Fig. 2B-D). At E14.5 *Scgb3a2* was strongly expressed in clusters of cells in proximal airways (Fig. 2C). Double ISH-IHC and confocal analysis of E14.5 lungs confirmed co-localization of *Scgb3a2* and NICD (Fig. 2E). Co-localization was not restricted to these cell clusters but was harder to detect elsewhere in the epithelium due to the weaker NICD signals.

We tested whether clusters of *Scgb3a2* positive cells were arising at sites of *Ascl1*-expressing cells, as seen for NICD. Sections from E13.5 –E18.5 lungs were labeled with a *Scgb3a2* riboprobe and an anti *Ascl1* antibody. At E14.5, *Scgb3a2* signals were present in the expected uniform and clustered patterns (Fig. 2F); 70-80% of the *Scgb3a2*-expressing clusters were associated with the *Ascl1*-expressing cell clusters. Confocal microscopy confirmed that cells expressing *Scgb3a2* or *Ascl1* were distinct and in direct contact. (Fig. 2G). Interestingly,

analysis of E13.5-E14.5 lungs showed a P-D pattern of pNEB formation in intrapulmonary airways, preceding the local appearance of *Scgb3a2* (Fig. 2H).

These data show that the pNEB-microenvironment at E14.5 consists of clusters of *Ascl1*-expressing cells and another cell population expressing high levels of NICD and *Scgb3a2*. No *Foxj1* labeling was detected in these cells at any of the stages studied. Therefore, we hypothesized that the NEB microenvironment is a niche for Clara cell precursors and examined the distribution of *Ccsp* in the NEB microenvironment at E18.5. However, simultaneous labeling of NICD/*Ccsp*/*Ascl1* at E18.5 demonstrated that cells clustered around NEBs had high levels of NICD but low to negligible levels of *Ccsp* (Fig. 2I-O). Three-color labeling of *Scgb3a2* (ISH)/*Ccsp* (ISH)/*Cgrp* (IHC) (Calcitonin gene-related peptide, another NE cell marker) confirmed that cells in the pNEB microenvironment continue to express *Scgb3a2* at this stage and have low to negligible levels of *Ccsp*. Our data suggested that cells associated with NEBs are a distinct set of Clara cell progenitors.

High levels of Uroplakin 3A (*Upk3a*) expression distinguishes secretory precursors in the NEB microenvironment

The absence of secretory cells in the airways of Notch signaling-deficient mice presented a unique opportunity to screen for additional markers enriched in the developing Clara cells. Thus, we compared the global gene expression profile of E18.5 lungs from control and mutant mice in which the *Rbpjk* gene was disrupted in the airway epithelium (*Shh-Cre;Rbpjk^{Flox/Flox}*, or *Rbpjk^{cnul}*)(18). As expected, genes associated with the Clara cell phenotype, such as *Ccsp*, *Scgb3a2* and *Cyp2f2* were expressed at significantly higher levels in control lungs (Fig. 3A). A comprehensive description of this screen will be reported elsewhere. Importantly, this screen identified Uroplakin 3a (*Upk3a*, Fig. 3A) as a putative marker of Clara precursors. *Upk3a* encodes a single-pass transmembrane domain-containing protein of the Uroplakin family that is expressed in the urinary bladder epithelium (19, 20). Mice deficient in *Upk3a* have compromised urothelial permeability but no phenotype has been described in the lung(19).

We examined *Upk3a* expression in control and *Rbpjk^{cnul}* mice by ISH (Fig. 3B,C). In E18.5 controls *Upk3a* was highly enriched in cell clusters in the proximal airways, although signals could be also detected at lower levels in scattered cells in the distal airway epithelium (Fig. 3B, bracket). This differed from the widespread expression patterns of *Scgb3a2* and *Ccsp* at E18.5 (Fig. 2). *Upk3a* signals were undetectable in airways of *Rbpjk^{cnul}* mice (Fig. 3C).

Developmental analysis of *Upk3a* expression using ISH and quantitative Real-time PCR (qPCR) detected signals at E12.5 (qPCR) and 14.5 (ISH), and showed increasing levels thereafter (Fig. 3D-F). ISH revealed clustered distribution from early stages and prompted us to investigate the relationship of *Upk3a*-expressing cells with pNEBs. Double ISH (*Upk3a*)/IHC (*Ascl1*) showed that *Upk3a*-expressing cells were juxtaposed to the *Ascl1*-labeled clusters from the earliest stages (Fig.3E-F). Quantitative analysis showed that between 70-80% of pNEBs at E14.5 were associated with *Upk3a* clusters. Next we investigated whether *Upk3a*-expressing cells were present in the NEB microenvironment in the adult lung. Double ISH/IHC using a *Upk3a*-riboprobe and an anti-*Cgrp* antibody showed at least 1-5 *Upk3a*-expressing cells in association with 50% of all NEBs examined (Fig. 3G).

Since *Cyp2f2* has been reported as marker for Clara cells (17) and was also identified by our expression profiling as downregulated in Notch-deficient airways, we characterized its developmental pattern of expression. ISH showed *Cyp2f2* expression throughout the epithelium of the trachea and extrapulmonary airways from E13.5 and expanded to distal airways at later

times (Suppl.Fig.1A,B). To determine the spatial relationships among *Scgb3a2*, *Upk3a*, *Cyp2f2* and pNEBs, serial sections were labeled with these riboprobes and subsequently stained with an anti-Ascl1 antiserum. Analysis of E14.5 lungs showed that the pNEB-associated cell clusters that typically express strong *Scgb3a2* and *Upk3a* signals, had little, if any, *Cyp2f2* (Suppl. Fig.1C-E). This contrasted with the strong *Cyp2f2* signals in neighboring *Scgb3a2* positive cells. At E18.5 this subpopulation could be distinguished by strong *Upk3a* but not by low *Cyp2f2* expression as seen at earlier times (Suppl. Fig. 1F).

The NEB microenvironment harbors a subset of Clara cell precursor in developing airways

Next we asked whether the features identified in the pNEB-associated cells were dependent on the pNEBs. Previous studies show that neither solitary NE cells nor NEBs form in Ascl1 null mice (13, 15). Given the small numbers of cells in the pNEB microenvironment and paucity of specific markers for these cells, we reasoned that the ablation of these cells would have escaped detection and reexamined the Ascl1 null mice. Analysis of these mutants at E14.5 showed that, in the absence of pNEBs, the clustered expression of NICD and *Scgb3a2* was abolished, although the weak, non-clustered signals remained in proximal airways (Suppl. Fig. 2A-D). At E18.5, the strong expression of NICD and *Scgb3a2* throughout the airway epithelium did not allow distinguishing differences between control and Ascl1 mutants.

We then investigated the impact of Ascl1 deletion on *Upk3a*. No *Upk3a*-labeled cell clusters were detected in Ascl1 null mutant lungs at E14.5 or E18.5 (Fig.3H-K). The selective loss of the *Upk3a*-labeled cell clusters was further supported by the presence of *Upk3a* signals in other structures (esophagus: Fig. 3I) or in the scattered cells outside the NEB microenvironment (Fig. 3K, inset) in Ascl1 mutants. The local impact of pNEB described here is agreement with the loss of SSEA-1-expressing cells in Ascl1 null mutants reported in the co-submitted manuscript by Morimoto et al. The Ascl1 phenotype contrasts with the generalized disruption of *Upk3a* that we found in the airways of *Rbpjk^{cnul}* mice (Fig. 3C). qPCR showed that *Upk3a* mRNA is abolished in *Rbpjk^{cnul}* lungs both at E14.5 and E18.5 (Fig. 3L). The observation is consistent with the inability to form Clara cells upon disruption of Notch signaling. In Ascl1 null mice, *Upk3a* expression was also markedly downregulated at E14.5 but only marginally decreased at 18.5 (Fig. 3L). The more dramatic reduction in *Upk3a* transcripts seen at E14.5 mutants was expected since at this stage *Upk3a*-expressing cells formed essentially around pNEBs. Later, the contribution of non-pNEB associated cells minimized the differences in *Upk3a* expression between control and Ascl1 mutants (see also Suppl. Fig.2 E-G for *Scgb3a2*). These results suggest that NEBs are required to induce if not maintain a population of cells expressing high levels of *Upk3a* in its microenvironment.

The identification of *Upk3a* as a marker enriched in pNEB microenvironment provided us with an opportunity to examine the fate of these cells. We investigated the fate of *Upk3a*-expressing cells in the airways during prenatal and adult life using an *Upk3aCreER^{T2}* transgenic mouse. A single dose of Tamoxifen (see methods, Figure 4A) was administered to *Upk3aCreER^{T2};Rosa26lacZ* dams 15.5 days post coitum. Offspring were analyzed at E18.5 and at postnatal day 60. As putative Clara cell precursors, we investigated the ability of *Upk3aCre*-labelled cells to give rise to Clara and ciliated cells (2). Thus, we performed double IHC/Xgal staining using antibodies against Foxj1, β Tubulin IV (ciliated), and Ccsp, followed by quantitative analysis. (Fig.4). At E18.5, while lacZ signal was detected in a small number of cells, few were double labeled with Ccsp and only a single cell was double-labeled with Foxj1. This showed that *Upk3a* lineage was largely uncommitted to either Clara or ciliated fates at this

stage and was consistent with our IHC/ISH studies. By contrast, analysis of adult lungs showed labeling in both ciliated and Clara cells at nearly similar proportion (Ccsp: $47.2 \pm 3.4\%$; β Tubulin: $45.3 \pm 4.0\%$) (Fig.4 J,K). The pool of cells that are lacZ positive, Ccsp negative and lacZ positive, β Tubulin negative may include cells that remained undifferentiated even in adults. Lineage-labeled cells were distributed throughout the airway epithelium and only a few of these cells were apposed to PNECs (Fig.B-G). Analysis using the NE marker PGP9.5 showed no colocalization with lacZ (total of 69 lacZ positive cells examined). Together our data suggest that during development the pNEB microenvironment harbors a population of less mature Clara cell precursors with equal potential to become Clara or ciliated cell (see discussion).

Notch signaling regulates expression of *Scgb3a2*, *Upk3a* and *Ccsp* by a transcriptional mechanism

To gain further insights into the mechanisms by which Notch signaling regulates gene expression in Clara progenitors, we examined the effect of loss or gain of Notch function on expression of genes at early stages, prior to the onset of Ccsp expression. We generated mice in which Notch signaling was disrupted (*Rbpjk*^{cnul})(18)) or constitutively activated in the lung epithelium using *ShhCre* and *Rosa-NICD* transgenes(12). Analysis of the *Scgb3a2* pattern in E14.5 *Rbpjk*^{cnul} lungs showed marked downregulation in extrapulmonary airways and negligible signals in intrapulmonary airways, including the cells in the pNEB microenvironment, which normally express strong *Scgb3a2* (Fig 5A-B; Fig.2). In contrast, E14.5 *ShhCreNICD* mice showed widespread expression of *Scgb3a2* in the airway progenitors (Fig. 5E). *Upk3a* expression was similarly modulated by Notch signaling (Fig. 5B, F). Interestingly, we did not detect expression of the late marker Ccsp in E14.5 lungs overexpressing NICD, but strong signals were present at E18.5 (Suppl.Fig. 3A, B). As evidenced by the morphology, NICD overexpression led to aberrantly enlarged airways. Nevertheless, these airways retained respiratory identity as they expressed Ttf1 (Fig.5C-D).

Based on the genetic data above and our evidence establishing *Scgb3a2* as an early Clara marker, we investigated whether Notch could directly regulate *Scgb3a2* transcription. A screen for *Rbpjk* binding sites 1kb region upstream to the Transcription Start Site (TSS) of the murine *Scgb3a2* promoter revealed high (YGTGRGAA) and low (RTGRGAR) affinity binding sites (Fig.5G)(21-23). For subsequent analysis we focused on the putative high affinity binding site. We performed electrophoretic mobility shift analysis (EMSA) using COS-1 cell nuclear extracts and oligonucleotides containing the *Rbpjk* high affinity binding sequence (intact, mutated); COS-1 cells are known to endogenously express *Rbpjk* (24). Detection of a DNA-protein band that was supershifted with an anti-*Rbpj* antibody confirmed that endogenous *Rbpjk* can bind to this site (Fig.5H). Next, we performed luciferase reporter assays using *Scgb3a2* promoter sequences -273 bp to the TSS containing either a control (WT) or a mutated *Rbpjk* high affinity site. Co-transfection with an NICD-containing plasmid resulted in minimal induction of reporter activity (<2-fold). This response was similar to that elicited by cotransfection of the same construct with an expression plasmid-containing Ttf1, a known transcriptional regulator of *Scgb3a2*. We conclude that despite the presence of a high affinity binding site in the promoter fragment, NICD expression is insufficient to induce reporter expression (Fig. 5I).

Interactions between Notch and other transcription factors have been implicated in the control of gene expression during development (21, 25). Moreover, synergistic regulation of the mouse *Scgb3a2* gene by Ttf1 and other transcription factors, such as C/EBP has been previously reported (26). We tested the possibility that NICD could act in concert with Ttf1 to transactivate

the *Scgb3a2* promoter (Fig.5I). Co-expression of Ttf1 and NICD dramatically increased reporter activity (over 40 fold). Importantly, introducing a mutation in the Rbpjk high affinity site (TTCTCACG to TTGTCTCG) nearly abolished this synergistic interaction (Fig.5I).

We extended our promoter analysis to other Clara cell-associated genes like *Upk3a* and *Ccsp*. Both genes have multiple Rbpjk and Ttf1 binding sites in their promoters (Suppl. Fig4 and 5). Reporter assays showed that both *Upk3a* and *Ccsp* were transactivated by NICD and Ttf1 in a synergistic manner, as observed for *Scgb3a2* (Suppl. Figs 4 and 5). Together, our data suggests a model in which Notch, in conjunction with locally expressed transcription factors, such as Ttf1, regulates gene transcription in Clara cell progenitors.

DISCUSSION

In this study we examined how Notch influences Clara cell fate specification in airway progenitors, and the influence of local microenvironment in generating diversity among Clara cell precursors during development. We provide evidence that commitment to a Clara cell fate occurs much earlier than the expression of *Ccsp* and we identify expression of *Scgb3a2* and Notch activation as early events in a program of Clara cell differentiation. Our *in vitro* assays show that Notch activation alone has a minimal effect in the transactivation of genes in Clara cell progenitors but is highly effective when combined with *Ttfl*. This context-dependency is of biological significance since genetic studies have shown that *Ttfl* is critical for the overall induction of respiratory cell fate, including secretory Clara cells (27, 28).

Ultrastructural studies of the developing airways show the pNEB microenvironment contains a distinct population of non-neuroendocrine, non-ciliated cells (5). Here we report that this population of pNEB-associated epithelial can be distinguished in molecular terms by the expression of markers associated with Clara cells such as NICD, *Scgb3a2*, *Upk3a*, *Cyp2f2* and *Ccsp*. Based on the marker that is most enriched and best distinguishes this population of cells, *Upk3a*, we undertook a lineage study to trace their fate in *Upk3aCreER^{T2}*; *Rosa26 lacZ* mice. We find that labeling at E15.5 results in *lacZ* expression in both Clara and ciliated cells of the adult airways at nearly the same proportion. Moreover, this lineage did not contribute to NE cells. Rawlins et al demonstrate that *Scgb1a1CreERTM*; *R26eYFP*-expressing cells labeled at E18.5 and examined in adult life contribute to both Clara and ciliated cells (2). Thus, our studies demonstrate that the *Upk3a*-expressing cells, despite expressing little *Ccsp*, exhibit the properties of a *Scgb1a1*-expressing Clara progenitor and implicate the pNEB microenvironment as a niche for Clara progenitors. It is likely that pNEBs are critical to specify or maintain the features of this subpopulation, however the identification of the NEB signals that mediate this process is beyond the scope of this work. Candidate signals present in NE cells potentially involved in these interactions include the Delta-like family of Notch ligands, or other currently uncharacterized *Ascl1* targets (15). Interestingly, lineage analysis of the *Scgb1a1*-expressing cells at E18.5 also demonstrates that these labeled cells contribute significantly to the ciliated lineage in the first three months of post-natal life but not significantly thereafter. In contrast, lineage labeling of *Scgb1a1*-expressing cells in the adult period identifies a population that contributes to the ciliated lineage throughout adult life (2). An explanation for this disparity is that the population of *Scgb1a1*-expressing cells that were labeled in the embryonic period differs from the population labeled during the adult period. The identification of the *Upk3a*-lineage derived Clara progenitors, that remain uncommitted through embryonic development, supports this possibility.

The spatial-temporal pattern of *Scgb3a2* we describe in murine airways, including its enrichment in clusters in the pNEB microenvironment is highly reminiscent of the CCSP pattern reported in developing airways of humans (29). Although SCGB3A2 has been reported in human neonatal lungs, no information is available on its pattern at early developmental stages in humans (14). A number of human conditions are associated with abnormal increase in NE bodies, including NE cell hyperplasia of infancy (NEHI), Diffuse idiopathic pulmonary neuroendocrine cell hyperplasia (DIPNECH) and Bronchopulmonary dysplasia (BPD). The aberrant expansion of neuroepithelial cells in these conditions is likely to have a profound impact in the local microenvironment, as shown by the increase in the NEB-associated clusters of CCSP-expressing cells in BPD lungs (29). Thus, further studies to better understand the mechanisms and

consequences of the cellular interactions in this microenvironment have potentially high clinical significance.

MATERIALS AND METHODS

Mouse strains and models

Developmental and adult expression studies were performed on CD1 mice (Charles River). Generation and genotyping of Rbpjk conditional knockouts and Ascl1 knockouts mice have been described previously (8, 30). Constitutive activation of Notch signaling in the developing airways was induced by breeding Shh cre/+ males to Rosa26 Notch1-ICD IRES GFP females (Jackson Laboratory); embryos expressing Notch1-ICD could be identified either by GFP expression or by diminutive tails. For lineage tracing experiments, Upk3acreER^{T2} (Jackson Laboratory) were bred to Rosa-26 LSL Lacz (Jackson Laboratory). For activation of β -galactosidase expression in embryonic lungs, an intraperitoneal injection of Tamoxifen in corn oil (1 mg to 40g body weight) was administered to pregnant mice at E15.5.

A detailed description of the reagents and methodologies (ISH, IHC, Real time PCR, EMSA, Site-directed mutagenesis, DNA transfections and Luciferase reporter assays) used in this work can be found in Supplemental Materials.

ACKNOWLEDGEMENTS

We thank FengZhi Shao for technical assistance and Mike Kirber, Narmada Khare and the members of the Cardoso lab and the Lung Development Group at the Pulmonary Center, BUMC for helpful discussions. We also thank Raphael Kopan and Mitsuru Morimoto for thought-provoking discussion and detailed comments on the manuscript. This work was funded by NIH-NHLBI (PO1 HL47049 to W.V.C.) and a BUMC start-up grant (to A.G.).

BIBLIOGRAPHY

1. Rawlins EL, *et al.* (2008) Epithelial stem/progenitor cells in lung postnatal growth, maintenance, and repair. *Cold Spring Harb Symp Quant Biol* 73:291-295.
2. Rawlins EL, *et al.* (2009) The role of Scgb1a1+ Clara cells in the long-term maintenance and repair of lung airway, but not alveolar, epithelium. *Cell Stem Cell* 4(6):525-534.
3. Reynolds SD & Malkinson AM (2010) Clara cell: progenitor for the bronchiolar epithelium. *Int J Biochem Cell Biol* 42(1):1-4.
4. Stripp BR, Maxson K, Mera R, & Singh G (1995) Plasticity of airway cell proliferation and gene expression after acute naphthalene injury. *Am J Physiol* 269(6 Pt 1):L791-799.
5. Hung KS (1982) Development of neuroepithelial bodies in pre- and postnatal mouse lungs: scanning electron microscopic study. *Anat Rec* 203(2):285-291.
6. Reynolds SD, Giangreco A, Power JH, & Stripp BR (2000) Neuroepithelial bodies of pulmonary airways serve as a reservoir of progenitor cells capable of epithelial regeneration. *Am J Pathol* 156(1):269-278.
7. Morimoto M, *et al.* (2010) Canonical Notch signaling in the developing lung is required for determination of arterial smooth muscle cells and selection of Clara versus ciliated cell fate. *J Cell Sci* 123(Pt 2):213-224.
8. Tsao PN, *et al.* (2009) Notch signaling controls the balance of ciliated and secretory cell fates in developing airways. *Development* 136(13):2297-2307.
9. Artavanis-Tsakonas S, Rand MD, & Lake RJ (1999) Notch signaling: cell fate control and signal integration in development. *Science* 284(5415):770-776.
10. Lai EC (2004) Notch signaling: control of cell communication and cell fate. *Development* 131(5):965-973.
11. Ilagan MX & Kopan R (2007) SnapShot: notch signaling pathway. *Cell* 128(6):1246.
12. Guseh JS, *et al.* (2009) Notch signaling promotes airway mucous metaplasia and inhibits alveolar development. *Development* 136(10):1751-1759.
13. Ito T, *et al.* (2000) Basic helix-loop-helix transcription factors regulate the neuroendocrine differentiation of fetal mouse pulmonary epithelium. *Development* 127(18):3913-3921.
14. Reynolds SD, Reynolds PR, Pryhuber GS, Finder JD, & Stripp BR (2002) Secretoglobins SCGB3A1 and SCGB3A2 define secretory cell subsets in mouse and human airways. *Am J Respir Crit Care Med* 166(11):1498-1509.
15. Borges M, *et al.* (1997) An achaete-scute homologue essential for neuroendocrine differentiation in the lung. *Nature* 386(6627):852-855.
16. Jain R, *et al.* (2010) Temporal relationship between primary and motile ciliogenesis in airway epithelial cells. *Am J Respir Cell Mol Biol* 43(6):731-739.
17. Zemke AC, *et al.* (2009) Molecular staging of epithelial maturation using secretory cell-specific genes as markers. *Am J Respir Cell Mol Biol* 40(3):340-348.
18. Tsao PN, *et al.* (2008) Gamma-secretase activation of notch signaling regulates the balance of proximal and distal fates in progenitor cells of the developing lung. *J Biol Chem* 283(43):29532-29544.
19. Hu P, *et al.* (2000) Ablation of uroplakin III gene results in small urothelial plaques, urothelial leakage, and vesicoureteral reflux. *J Cell Biol* 151(5):961-972.

20. Liang FX, *et al.* (2001) Organization of uroplakin subunits: transmembrane topology, pair formation and plaque composition. *Biochem J* 355(Pt 1):13-18.
21. Schwanbeck R, Martini S, Bernoth K, & Just U (2011) The Notch signaling pathway: molecular basis of cell context dependency. *Eur J Cell Biol* 90(6-7):572-581.
22. Ong CT, *et al.* (2006) Target selectivity of vertebrate notch proteins. Collaboration between discrete domains and CSL-binding site architecture determines activation probability. *J Biol Chem* 281(8):5106-5119.
23. Morel V & Schweisguth F (2000) Repression by suppressor of hairless and activation by Notch are required to define a single row of single-minded expressing cells in the *Drosophila* embryo. *Genes Dev* 14(3):377-388.
24. Lu FM & Lux SE (1996) Constitutively active human Notch1 binds to the transcription factor CBF1 and stimulates transcription through a promoter containing a CBF1-responsive element. *Proc Natl Acad Sci U S A* 93(11):5663-5667.
25. Bray S & Bernard F (2010) Notch targets and their regulation. *Curr Top Dev Biol* 92:253-275.
26. Tomita T, *et al.* (2008) CAATT/enhancer-binding proteins alpha and delta interact with NKX2-1 to synergistically activate mouse secretoglobin 3A2 gene expression. *J Biol Chem* 283(37):25617-25627.
27. Kimura S, *et al.* (1996) The T/ebp null mouse: thyroid-specific enhancer-binding protein is essential for the organogenesis of the thyroid, lung, ventral forebrain, and pituitary. *Genes Dev* 10(1):60-69.
28. Minoo P, Su G, Drum H, Bringas P, & Kimura S (1999) Defects in tracheoesophageal and lung morphogenesis in Nkx2.1(-/-) mouse embryos. *Dev Biol* 209(1):60-71.
29. Khor A, Gray ME, Singh G, & Stahlman MT (1996) Ontogeny of Clara cell-specific protein and its mRNA: their association with neuroepithelial bodies in human fetal lung and in bronchopulmonary dysplasia. *J Histochem Cytochem* 44(12):1429-1438.
30. Guillemot F, *et al.* (1993) Mammalian achaete-scute homolog 1 is required for the early development of olfactory and autonomic neurons. *Cell* 75(3):463-476.
31. Liu G, Amin S, Okuhama NN, Liao G, & Mingle LA (2006) A quantitative evaluation of peroxidase inhibitors for tyramide signal amplification mediated cytochemistry and histochemistry. *Histochem Cell Biol* 126(2):283-291.

FIGURE LEGENDS

Figure 1: Spatial pattern of Notch activation in the developing airways. (A-G) Labeling for cleaved Notch1 (NICD, red) and Ascl1 (green) indicates that Notch signaling is activated in the airways a few days earlier than Ccsp expression is detected (E15.5, 14) and that it is active in the NEB microenvironment from early stages. (A-B) Low levels of NICD were detected at E12.5 in trachea (Tr) and main bronchi (arrow) but no signal was detected in distal (dl) airways (shown at higher resolution B). Note strong NICD staining in the vasculature (V). (C-F) At E14.5 NICD labeling was more abundant in both the extrapulmonary airways (Tr in C, higher magnification in D) and proximal intrapulmonary airways (C, higher magnification in E), but no labeling was detected in distal airways (inset in C). (F) Clusters of strong NICD labeling in the proximal intrapulmonary airways at E14.5 are associated with clusters of Ascl1-expressing cells (arrows, airway outlined in white). Note the solitary Ascl1-expressing cells (arrowhead) further away are not associated with strong NICD labeling (F). (G) At E18.5 widespread labeling of NICD was detected in the intrapulmonary airways including the NEB microenvironment (arrow). Lu=lung, L=lumen. Scale bar=10 μ m.

Figure 2: *Scgb3a2* expression correlates with NICD and identifies a distinct subpopulation of Clara-like progenitors associated with presumptive neuroepithelial bodies (pNEBs). (A-D) Time-course of *Scgb3a2* expression revealed a pattern similar to that of NICD (Fig. 1). *Scgb3a2* was first detected in the trachea (Tr) at E12.5 (A) and in the intrapulmonary airways from E13.5-E14.5 (B-D). At E18.5 (D) *Scgb3a2* expression was widespread and detected in both trachea (Tr) and terminal bronchiole (TB). Clusters of cells with strong signal could be discerned at E13.5-E14.5 (B, C, inset in C, arrows). (E) Colocalization of *Scgb3a2* and NICD was readily observed in these cell clusters (arrows, lumen of the airway is indicated (L)). (F) Double *Scgb3a2* ISH/Ascl1 IHC revealed *Scgb3a2*-labeled clusters (F, right panel) juxtaposed to Ascl1-expressing pNEBs. Inset in F shows that *Scgb3a2*-expressing cells (blue) have a clear nucleus not labeled by anti-Ascl1 (brown). No Ascl1-expressing cells were detected in the trachea (F, left panel). (G) High-resolution optical section showing that luminal *Scgb3a2*-expressing cells (ISH, red) could be distinguished from basal Ascl1-expressing cells (IHC, green). (H) *Scgb3a2* and Ascl1 double labeling at E13.5 suggests that the formation of Ascl1-clusters (distal, arrows) precedes formation of *Scgb3a2*-Ascl1 dual clusters. (I-O) Analysis of *Ccsp* and *Scgb3a2* expression at E18.5 suggested that the cells associated with pNEBs may be a distinct subpopulation of Clara precursors. (I-K) Labeling of NICD (red, shown separately in J), *Ccsp* (white, shown separately in K) and Ascl1 (green) showed that the cells in the NEB microenvironment are NICD-positive but express low (arrow) to negligible levels of *Ccsp* at this stage. Cells with both NICD and *Ccsp* were abundant away from the NEB microenvironment (I). (L-O) Triple-labeling for *Scgb3a2* (ISH, red, shown separately in M), *Ccsp* (ISH, green, shown separately in N) and *Cgrp* (IHC, blue, shown separately in O) at E18.5 showed that cells apposed to pNEBs express *Scgb3a2* and low *Ccsp* (arrowhead) and some have *Scgb3a2* but negligible *Ccsp* (arrow). Elsewhere *Scgb3a2* and *Ccsp* signals are strong and colocalized (L).

Figure 3: High levels of Uroplakin 3A (*Upk3a*) expression distinguishes secretory precursors in the pNEB microenvironment (A) Profiling of E18.5 control and Notch signaling-deficient (*Rbpj^{cnul}*) lungs identified known markers for secretory cells and implicated *Upk3a* as a novel marker. (B-C) ISH at E18.5 in control lungs revealed that *Upk3a* was highly

enriched in clusters of cells in the proximal airways (C, arrow) and expressed at low-levels in scattered cells in distal airways (C, bracket). No signal was detected along the airway axis in *Rbpj*^{cnull} airways (Tr, trachea). (D) qPCR analysis showed that *Upk3a* levels can be detected at E12.5 and increase throughout development. (E-F) *Upk3a* transcripts were detected by ISH from E14.5 onwards in cell clusters juxtaposed to *Ascl1*-expressing cells (E, F, boxed areas shown at higher magnification in insets). Some expression away from clusters was detected from E16.5 onwards (F, bracket). *Upk3a* expression was also detected in a few cells in the adult airways (G, arrow) frequently juxtaposed to *Cgrp*-expressing NEBs (inset). (H-K) *Upk3a* expression was perturbed in *Ascl1* null (*Ascl1*^{-/-}) lungs. Clusters of high *Upk3a* expression were detected in control at both E14.5 (H) and E18.5 (J) but not in mutant lungs at either time point (I,K, circled regions; note expression of *Upk3a* is detected in the esophagus in the mutant at E14.5 (I, eso)). Rare *Upk3a*-expressing cells (non-clustered) could still be seen in the E18.5 *Ascl1* null mutant (K, inset). (L) qRT-PCR analysis of *Upk3a* expression in *Rbpjk*-deficient and *Ascl1* mutants at E14.5 and E18.5 showing that *Upk3a* expression is dependent on both Notch signaling and *Ascl1*.

Figure 4: Lineage-analysis of *Upk3a*-expressing cells at E15.5 reveals that these cells are precursors of Clara and ciliated cells. (A) Experimental protocol for the induction and harvest of tissue from the *Upk3acreER*^{T2} X *Rosa26lacZ*. (B-E) *Upk3a*-lineage derived cells (blue) are distributed along the proximal-distal axis (airways counterstained with Fast Red) in clusters and as solitary cells (B, arrows). Regions 1, 2, 3 in B are shown at higher magnification in C-E. (F-G) Double labeling of X-gal stained preparations for PGP9.5 shows that *Upk3a*-lineage derived cells (arrows) are not in close association with NEBs (arrowheads) though rare examples of apposition are observed (G). Note that *LacZ* (arrow) and PGP9.5 (arrowhead) expressing cells are distinct from another. (H-I) *Upk3a*-expressing cells labeled at E15.5 contribute to Clara and Ciliated lineages in adults Double labeling of X-gal stained preparations for *Ccsp* (H) and β Tubulin (I) demonstrate that these cells contribute to both Clara (H) and ciliated (I) lineages. (J-K) Quantitation of the numbers of X-gal stained cells that co-label for Clara and ciliated markers at E18.5 (*Ccsp*, *Foxj1*, n=156 airways) and in adults (*Ccsp*, β Tubulin, n=501 airways). The *Upk3a*-lineage derived cells are mostly uncommitted to either Clara or ciliated fates at E18.5 but differentiate into these lineages in the peri-natal period (proportions of ciliated and clara cells in adults is shown graphically in K, mean+/-sem). See supplementary text for methods.

Figure 5: Notch-dependent regulation of secretory cell-associated genes. (A-F) Analysis of Notch gain and loss-of-function in E14.5 airways *in vivo* (A,B) Disruption of Notch signaling in *Rbpj*^{cnull} mutants disrupts expression of *Scgb3a2* and *Upk3a*. Comparable segments of the intrapulmonary airways in A, B (encircled by grey lines) evidence negligible expression of both markers in *Rbpj*^{cnull} lungs. Residual low-level expression of *Scgb3a2* was detected in the extrapulmonary airways of mutants only after prolonged ISH exposure (A, arrow). Double *Scgb3a2* ISH/*Ascl1* IHC shows that specification of pNEBs was unaffected in *Rbpj*^{cnull} mutants but no *Scgb3a2* was detected in surrounding cells (A, inset, arrowhead). (C-F) *Shhcre* driven NICD perturbed lung architecture (compare distribution of *Ttf1* in C, D) and resulted in widespread expression of *Scgb3a2* and *Upk3a*. (G-H) *In vitro* analysis of the role of Notch signaling in the regulation of the *Scgb3a2* promoter. (G) Schematic showing presumptive *Rbpjk* binding sites (high affinity site: red arrow; low affinity site: grey arrow) in the *Scgb3a2* promoter

1 kb upstream to the transcription start site. Right panel: sequence of a -273 bp fragment of the *Scgb3a2* promoter showing putative Rbpjk (red) and TTF1 (green) binding sites. (H) Validation of the predicted high affinity Rbpjk binding site in the *Scgb3a2* promoter by EMSA. An anti-Rbpjk antibody supershifted the labeled oligonucleotide containing the putative high affinity binding site (CTRL, Lane+ab). Note that the band that is supershifted by anti-Rbpjk was competed by co-incubation of the labeled oligonucleotide with an unlabeled CTRL oligonucleotide (cognate) but not competed by co-incubation with an unlabeled mutant oligonucleotide lacking the high affinity binding site (MUT, sequences shown below). (I) Luciferase assay examining the sufficiency of NICD and Ttf1 in the transactivation of the *Scgb3a2* promoter. NICD expression alone did not significantly transactivate the *Scgb3a2* promoter but co-expression of NICD and Ttf1 synergistically upregulated reporter expression. This synergistic upregulation was abolished when the high affinity Rbpjk binding site was mutated (-273mut, see G).

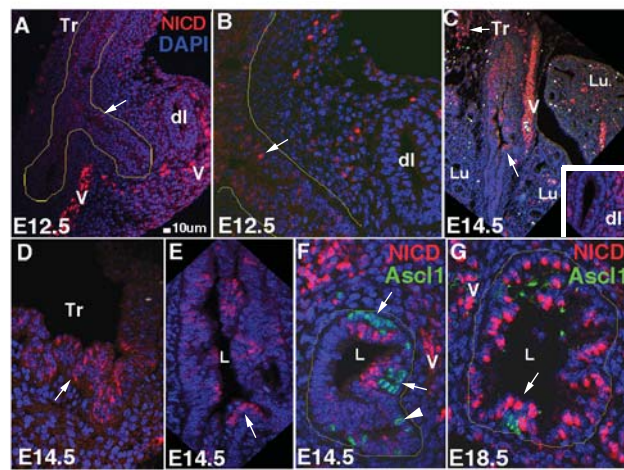


FIGURE1, Guha et al

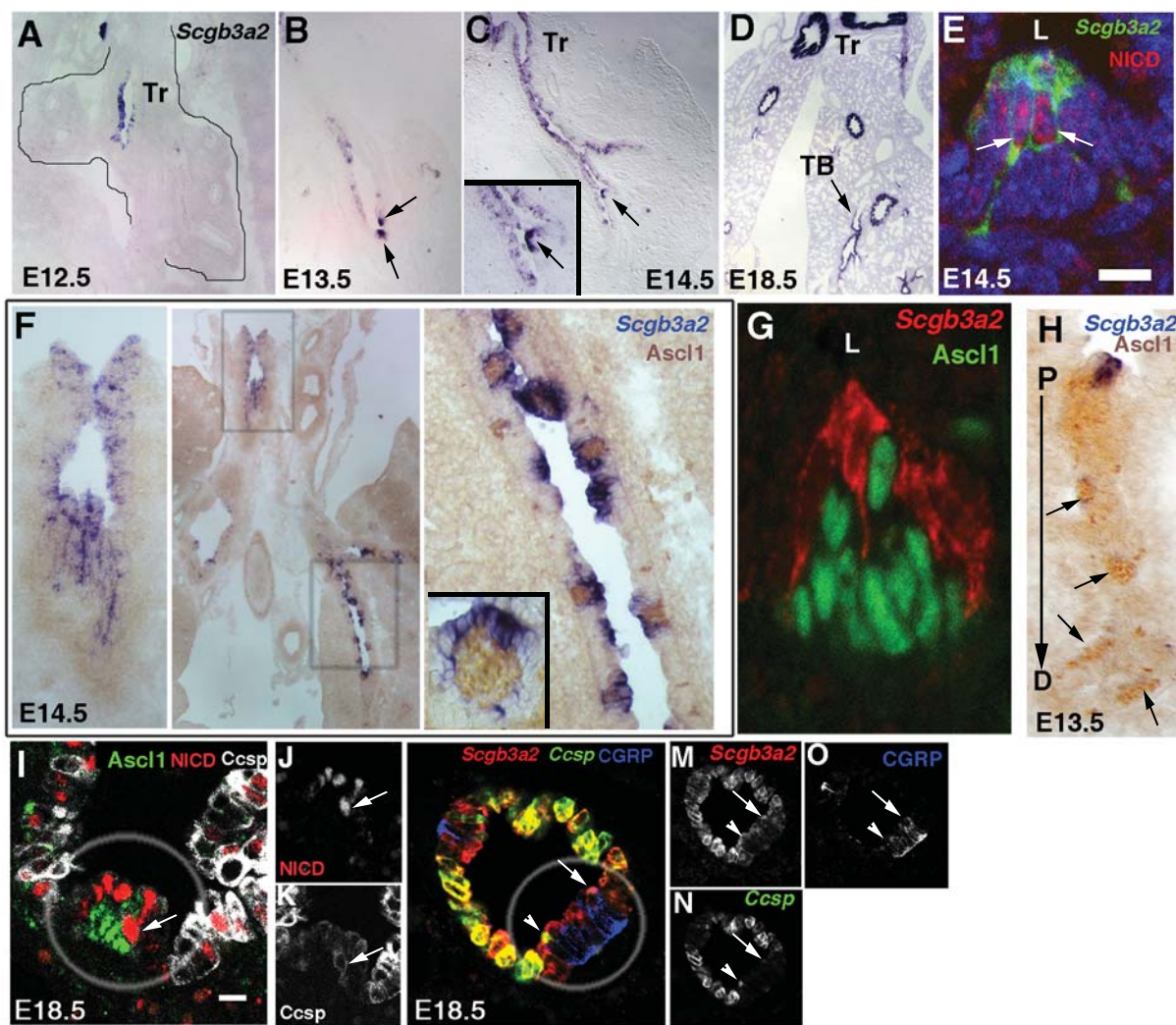


FIGURE 2, Guha et al

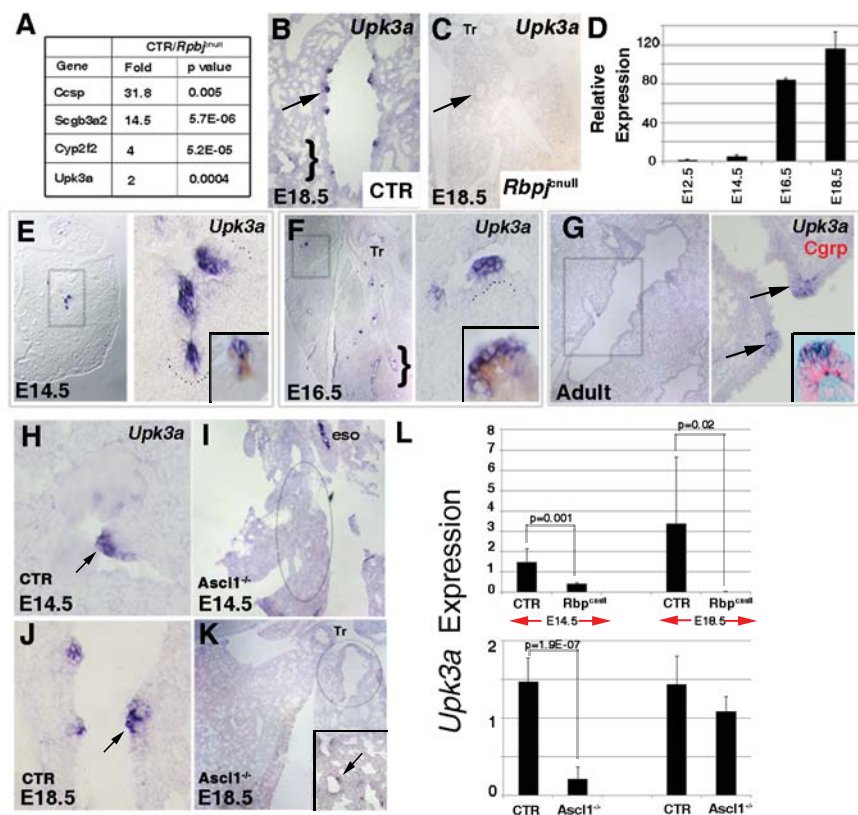


FIGURE 3, Guha et al

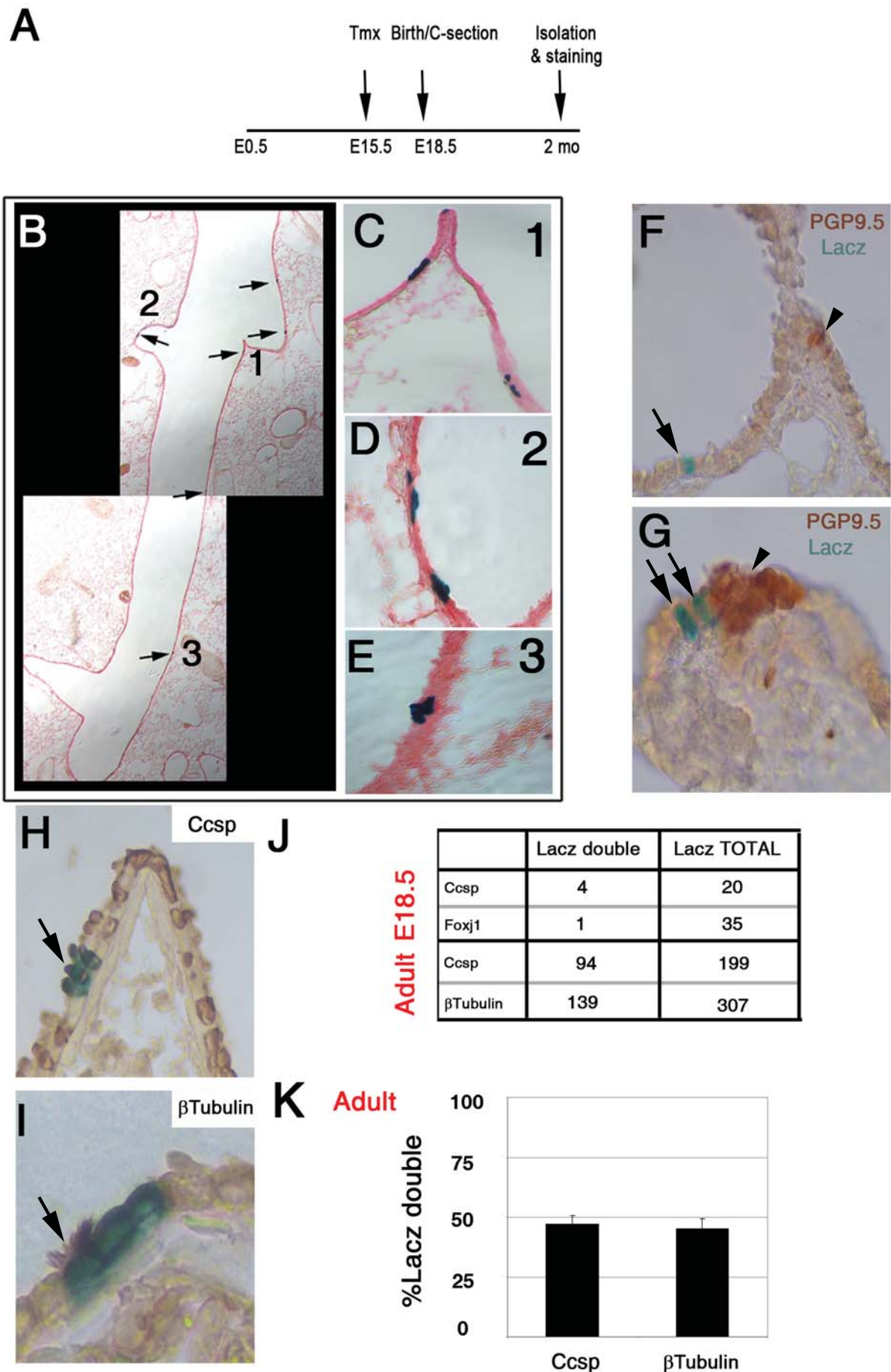


FIGURE 4, Guha et al

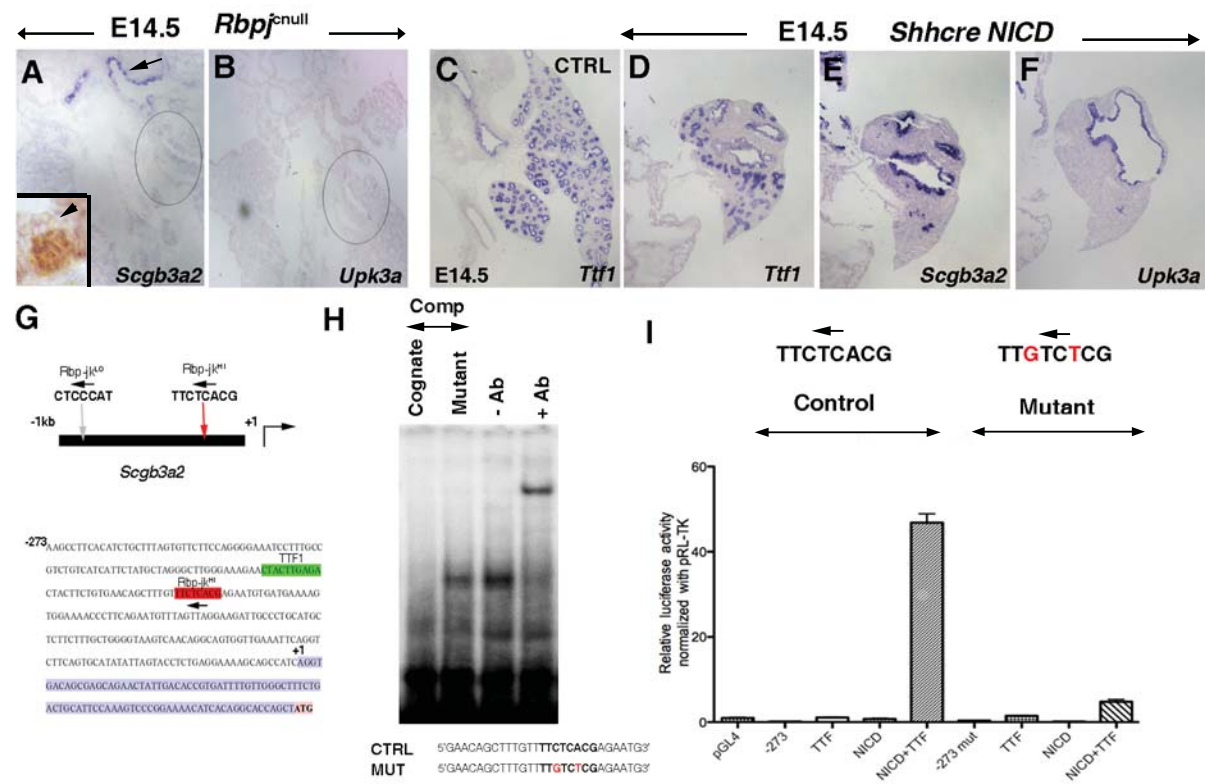


FIGURE 5, Guha et al